Carbohydrate Polymers 88 (2012) 1272–1280

Contents lists available at SciVerse ScienceDirect

Carbohydrate Polymers

journal homepage: www.elsevier.com/locate/carbpol

# Modified cellulose films with controlled permeatability and biodegradability by crosslinking with toluene diisocyanate under homogeneous conditions

Xiaoyun Qiu[a], Shuming Tao[b], Xueqin Ren[a,*], Shuwen Hu[a,**]

[a] Department of Environmental Sciences & Engineering, College of Resources & Environmental Sciences, China Agricultural University, Beijing 100193, PR China
[b] Department of Plant Nutrition, College of Resources & Environmental Sciences, China Agricultural University, Beijing 100193, PR China

ARTICLE INFO

*Article history:*
Received 21 November 2011
Received in revised form 3 February 2012
Accepted 3 February 2012
Available online 10 February 2012

*Keywords:*
Cellulose film
Crosslink
Permeation
Biodegradable

ABSTRACT

Microcrystalline cellulose was modified by crosslinking with toluene diisocyanate under homogeneous phase in N,N-dimethylacetamide/LiCl solvent system. Modified cellulose films were prepared by solution casting method and their hydrophobicity, thermal stability, permeability, and degradability were characterized. The hydrophobicity, thermal stability, and mechanical properties of the films were improved by crosslinking according to the comprehensive results. The permeation rate of urea dropped rapidly from 107.7 mg/(cm$^2$ h) to 0.88 mg/(cm$^2$ h) with toluene diisocyanate/microcrystalline cellulose (TDI/MCC) increasing. Biodegradability of the films was examined in both controlled compost extract and natural cultivated soil. Comprehensive results including $CO_2$ emission, scanning electron microscope (SEM) and attenuated total reflection infrared (ATR-IR) demonstrated that the films were biodegradable and the biodegradability decreased with TDI/MCC increasing. The results indicated that both permeation capability and biodegradability of the cellulose films can be optimized based on requirements.



## 1. Introduction

The requirements of environmental protection, preservation of natural resources, and increased pressure from attended stringency of laws lead to the blooming development of natural materials particularly for renewable raw materials (Jawaid & Khalil, 2011). Cellulose, a dominant component in the vast majority of plant forms, having an annual production which is estimated to be around $1.0 \times 10^{11}$ t (French et al., 2004; Klemm, Philipp, Heinze, Heinze, & Wagenknecht, 1998, chap. 1), is a promising resource for developing renewable products due to its abundance and biodegradability.

In order to improve processing ability, chemical modification of cellulose is performed to provide different varieties of cellulose derivatives. Cellulose derivatives, which are in general robust, reproducible, recyclable and biocompatible (Conner, 1995), have been widely studied and utilized as fiber, film and gel-based materials intensively (Bras, Vaca-Garcia, Borredon, & Glasser, 2007; Philipp & Schempp, 2009). Esterification, etherification, acetalization, and oxidation are the most important reaction types of cellulose, while chemical modification with isocyanates presents some unique properties due to: (i) relatively high reaction rates; (ii) absence of secondary products; and (iii) chemical stability of urethane moiety (Siqueira, Bras, & Dufresne, 2010). Different kinds of isocyanates have been used to modify cellulose (Amarasekara & Owereh, 2009; Gironès et al., 2007, 2008; Siqueira et al., 2010), and these carbamate derivatives of cellulose have been explored for applications as film materials in the fields of hemodialysis and gas permeation (Diamantoglou, Platz, & Vienken, 1999; Khan, Shiotsuki, Nishio, & Masuda, 2008).

Applications of cellulose films in anion exchange (Schmitt, Granet, Sarrazin, Mackenzie, & Krausz, 2011; Tatárová, Fáberb, Denoyelc, & Polakoviča, 2009), separation (Grainger & Hägg, 2007; Pan, Hamad, & Straus, 2010; Wang, Yang, Luo, & Dai, 2009; Zaghbani, Hafiane, & Dhahbi, 2007), controlled release (Bodhibukkana et al., 2006; Valente et al., 2005; Wu et al., 2010), metal ion absorption (Chen et al., 2009; Tian et al., 2011), and water treatment (Liu, Zeng, Tao, & Zhang, 2010; Lqbal, Kim, Yang, Baek, & Yang, 2007) *etc*., have been intensively exploited in recent years. Cellulose films, obtained by regeneration (Liu et al., 2010), crosslinking (Schmitt et al., 2011), and grafting (Tatárová et al., 2009), possessing unique features such as eco-friendly, highly resistant to mechanical strain, easily modified into porous films, and stable in most inorganic/organic solutions, are essential for industrial application.

*Abbreviations:* MCC, microcrystalline cellulose; TDI, toluene diisocyanate; DMAc, N,N-dimethylacetamide; TGA, thermal gravimetric analysis; SEM, scan electron microscope; FT-IR, fourier transform infrared spectroscopy; ATR-IR, attenuated total reflection infrared; WRVs, water retention values; UV, ultraviolet spectrophotometry; PE, polyethylene.

* Corresponding author. Tel.: +86 10 62733407; fax: +86 10 62731016.
** Corresponding author. Tel.: +86 010 62731255; fax: +86 010 62731016.
*E-mail addresses:* renxueqin@cau.edu.cn (X. Ren), shuwenhu@cau.edu.cn (S. Hu).

0144-8617/$ – see front matter © 2012 Elsevier Ltd. All rights reserved.
doi:10.1016/j.carbpol.2012.02.007

Meanwhile, the research of degradation characterizations has been one of the focuses of cellulose studies these years (Glaus & Van Loon, 2008; Łojewski et al., 2010; Pala, Mota, & Gama, 2007; Wilson, 2009). The conditions of cellulose degradation, such as aerobic or anaerobic, and the microorganisms, kinetics, and mechanisms of cellulose degradation process have been comprehensively investigated. Degradation behaviors of some cellulose derivatives have also been studied (Erkselius & Karlsson, 2005; Ouajai & Shanks, 2005; Tomšič, Simončič, Orel, Vilčnik, & Spreizer, 2007; Yuan, Yuan, Zhang, & Xie, 2007), yet the influences of chemical modification on both biodegradability and controlled permeation have not been discussed and little is known about that. Besides, unmodified cellulose degraded too fast (Glaus & Van Loon, 2008; Tomšič et al., 2007), so the biodegradability should be adjusted for further applications.

Variegated properties of cellulose films are highly requested in different fields, and here we present a novel way to produce cellulose films with controllable permeability and degradability as request. In this work, cellulose derivatives combined controlled biodegradability and permeability were designed by modifying cellulose with toluene diisocyante (TDI) under homogeneous conditions using DMAc/LiCl as the solvent system. Afterwards, films were formed by solution casting method and used to study their permeation and biodegradation properties. Furthermore, the present work was supposed to reveal the influences of TDI modification on both permeation and degradation properties of cellulose films. The potential applications of these films are controlled release material for agricultural agents, such as fertilizers and pesticides, and membrane materials for water treatment and other industries.

## 2. Experimental

### 2.1. Materials

Microcrystalline cellulose (MCC) with a degree of polymerization of 210–240, lithium chloride monohydrate (analytical pure) and DMAc (chemical pure) were purchased from Sinopharm Chemical Reagent Co., Ltd. TDI was purchased from Shenyang Chemical Reagent Factory and used as received. MCC was dried in an air dry oven overnight at 80 °C before use. LiCl was dried in a vacuum-oven at 200 °C for 2 h prior to use. All other reagents were purchased from Beijing Chemical Reagents Company except with special note and used without any further treatment. Distilled water was used for all the experiments.

### 2.2. Preparation of cellulose solution

Cellulose cannot be dissolved in common solvents and chemical modification of cellulose in heterogeneous condition are generally impeded with regard to reaction rate, degree of conversion and site of conversion, being controlled by the supramolecular order and the fibrillar architecture of the polymer (Klemm et al., 1998, chap. 2). DMAc/LiCl solvent system was chosen and cellulose dissolving process was performed according to the method reported earlier (Dupont, 2003). In brief, 200 mL DMAc was introduced into a 250 mL, four-necked flask equipped with a $N_2$ inlet, a stirrer, a thermometer, and a condenser, which was heated to 150 °C for 10 min through vigorous stirring. 5.0 g MCC was added and activated at 150 °C with refluxing DMAc for 30 min. After activation, the temperature was decreased from 150 °C to 100 °C and allowed to stabilize for 20 min. Then 8.0 g LiCl was added into the flask. The temperature was kept at 100 °C for 40 min and then cooled to room temperature to obtain a completely dissolved cellulose solution, which was slightly yellowish and sticky.

### 2.3. Modification of cellulose and film forming

In order to incorporate carbamate, cellulose films with different crosslinking densities were prepared at five weight ratios of TDI/MCC: 0.00/1, 0.65/1, 1.30/1, 1.95/1, 2.60/1. For simplicity, above compositions were referred to as $C_0$, $C_1$, $C_2$, $C_3$, and $C_4$. 30 mL cellulose solution with 0.48 g cellulose was introduced into a flask and TDI was dissolved in DMAc with a concentration of 0.3 g/mL. The solution was stirred at room temperature for 5 min and then cast onto a square teflon plates with dimension of 20 cm × 20 cm. After exposure in air for 6 h at ambient temperature, the teflon plates were removed in an air dry oven overnight at 80 °C. Then formed films were peeled off and washed with distilled water three times to wash away remaining LiCl on the surface. Finally, the films were dried in a vacuum-oven at 80 °C for another 4 h to get the final films with thickness around 60 μm. The reaction between cellulose and TDI is illustrated in Scheme 1.

### 2.4. Chemical characterization

FT-IR spectra were recorded in the range of 500–4000 $cm^{-1}$ with a resolution of 8 $cm^{-1}$ on Nicolet NEXUS-470 FT-IR equipment (Madison, USA). For the transmission mode, the samples were ground in a mortar with FT-IR grade KBr (Aldrich) and then compressed into pellets. All the spectra were collected and processed

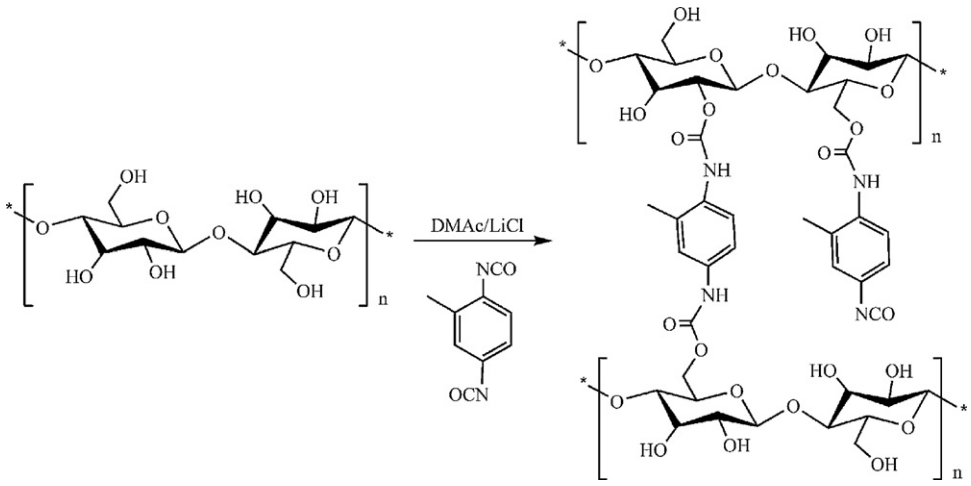


**Scheme 1.** Illustration of the crosslinking reaction between cellulose and TDI. Reaction conditions: 80 °C in air dry oven overnight.

with the Thermo Nicolet's OMNIC® Software accompanied with the instrument.

For analysis of degradation properties, attenuated total reflection infrared (ATR-IR) spectra of cellulose films were obtained. The spectra were recorded in the range of 675–4000 $cm^{-1}$ with a resolution of 8 $cm^{-1}$ on Nicolet NEXUS-470 FT-IR equipment (Madison, USA).

### 2.5. Scanning electron microscope (SEM) analysis

Surface morphologies were examined by SEM using a JEOL JSM 5400 scanning microscope from JEOL Ltd. Co. (Tokyo, Japan) at an accelerating voltage of 15 kV. Samples were mounted on metal stubs and coated with gold–palladium by Denton Vacuum Desc II.

### 2.6. Thermo-gravimetric analysis (TGA)

A thermal weight change analysis was carried out using TGA Q50 V20.6 Build 31 from TA Instruments (New Castle, USA) to measure the amount and rate of change in weight of the films as a function of increasing time and temperature. The samples (around 5.5 mg) were heated in the furnace up to 800 °C at heating rate of 10 °C/min in air. The percentage of weight loss was plotted against temperature.

### 2.7. Water retention values (WRVs)

Films were cut into small pieces with equal size and weight, and then soaked in distilled water for 24 h. The surface water was carefully wiped out with filter paper before the films were subjected to weighing. All the procedures proceeded at room temperature. WRVs were calculated as the amount of absorbed water related to dry film mass as follows:

$$\text{WRVs } (\%) = \frac{W_t - W_0}{W_0} \times 100 \quad (1)$$

where $W_t$ is the weight of films after soaking, and $W_0$ is the dry weight of films before soaking. The obtained results were the average values of three duplicates.

### 2.8. Contact angle measurement

Contact angles were determined by the pendant drop method with a water drop of 3 μL and an optical contact angle meter SL 100B from Solon Information Technology Co., Ltd. (Shanghai, China) at room temperature and ambient humidity. All contact angles were measured on both sides of the drop by the ellipse-fitting calculation method. Each contact angle reported here was the average value after minimum four measurements.

### 2.9. Tensile strength measurement

The cellulose films were cut into dumbbell-shaped samples. Four tests were performed on each film, at room temperature, using an electronic universal testing machine C43 (Shenzhen, China) at a stretching speed of 2 mm/min. Characteristic parameters of the dumbbell-shaped samples were a gauge length of 25 mm, a width of 5 mm and a thickness of 60 μm.

### 2.10. Characterization of permeation properties

Experiments were carried out in a Transdermal Diffusion Device TK-6H from Shanghai KaiKai Science and Technology Trade Ltd. Co. (Shanghai, China), which was made up of six diffusion cells attached to a multi-stirrer with clamps. Each diffusion cell was built up by two detachable glass compartments with two sampling inlets, a stirrer, and an interlayer. Films with an average thickness of 60 μm were allowed to soak in distilled water overnight before use and cut into pieces with diameters about 30 mm. The film under study was sandwiched between two compartments with an effective diffusion area of 5.5 $cm^2$ and the compartments were clamped together with a tight steel clip. One compartment of the cell (the donor cell) was filled with 20 mL saturated urea solution and the other (the receiving cell) with 20 mL distilled water. The urea solution was kept saturated throughout the experiment by adding urea granules. The interlayer of each compartment was connected to a thermostatic water-circulator bath from Shanghai Bilon Instruments Co., Ltd. (Shanghai China). And the experiments were conducted with circulated water at a constant flow rate of 4 L/min, 30 °C, and a stirring speed at 200 rpm. Urea permeated from the donor cell into the receiving cell due to the concentration gradient across the films between the two cells. The urea content in the receiving cell was sampled every 1 h for UV analysis and another 20 mL of distilled water was added for replenishment. The urea concentration was determined by UV according to chromogenic reaction of urea with p-dimethylaminobenzaldehyde at wavelength of 426 nm (Zou, Wang, Dai, Zhou, & Ma, 2006). The obtained results were the average values of three duplicates.

The fluxes of urea permeating through films ($J$) were calculated as following formula:

$$J = \frac{M_t}{A \times t} \quad (2)$$

where $M_t$ is the amount of urea that permeated through the films at time $t$ (mg), $A$ is the actual diffusion area of films ($cm^2$), and $t$ is the time of the diffusion experiment.

### 2.11. Characterization of biodegradation properties

#### 2.11.1. Biodegradation in controlled composting environment

The biodegradable properties of films were characterized according to the International Standard ISO 14852 (1999). Films (0.5 ± 0.01 g) were cut into small pieces and introduced into testing vessels filled with 200 mL standard test medium, vaccinated with 10 g/100 mL of extracted finished compost from municipal solid waste. The testing vessels were put into a WE-2 water bath shaker from Tianjin Honour Instrument Co., Ltd. (Tianjin, China) at 45 °C at a shaking speed of 95 rpm. $CO_2$ trapping bottles were removed and replaced by new ones every two days at the first ten days, every five days afterwards, and $CO_2$ content in the trappers was determined by neutralization–titration as described by ISO 14852 (1999). Control experiments (CK) with no film added in testing vessel and experiment with 0.5 ± 0.01 g polyethylene (PE) in the testing vessels were conducted simultaneously. Each sample with two replicates was conducted for repeatability.

#### 2.11.2. Biodegradation in natural cultivated soil environment

Films were also buried in cultivated soil to characterize biodegradation behavior outdoors. Cellulose films with different crosslinking density and PE, weighted 0.2 ± 0.02 g respectively, were cut into small pieces with equal size, and three replicates of each sample were put into nylon net bags with mesh size of 100. The sample bags were buried in sandy loam located at Shangzhuang experimental station of China Agricultural University, Haidian District, Beijing. The physico-chemical properties of the soil were referred to an earlier publication (Hu et al., 2006). Samples were fetched out at intervals (1, 4, 8, 12, 16, 20, 24 months) and carefully washed with tap water followed by distilled water for several times. Before submitting for further characterization, the samples were cleaned in ultrasonic bath for another 20 min and air dried at 80 °C overnight.

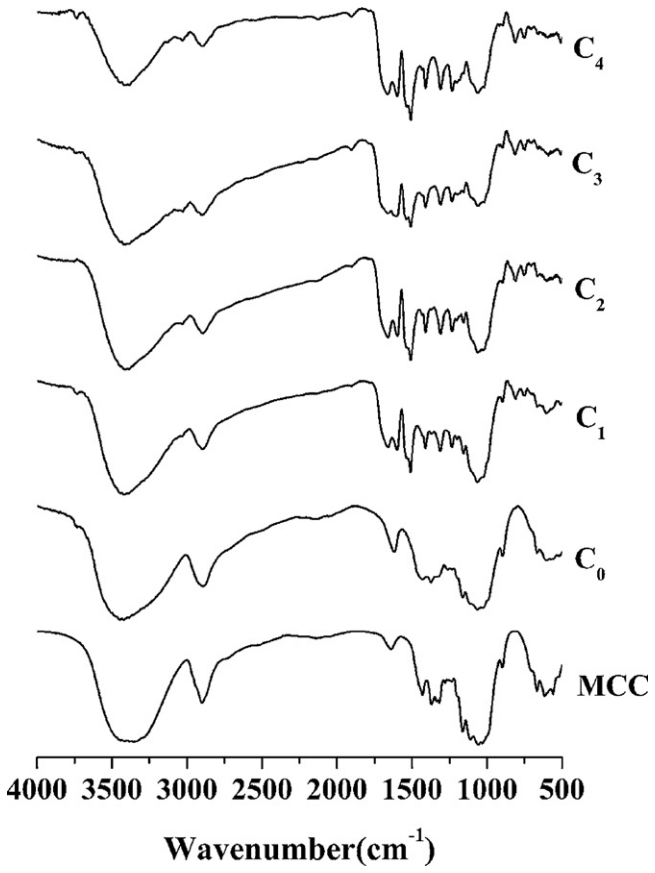


**Fig. 1.** FT-IR spectra of unmodified MCC and TDI modified cellulose with different crosslinking density.

Mass-loss ratio of the films was calculated as the amount of weight loss per dry film mass. ATR-IR and SEM were also performed to characterize degradability of films.

## 3. Results and discussion

### 3.1. FT-IR analysis

Fig. 1 shows the FT-IR spectra of MCC films before and after TDI modification. $C_0$, $C_1$, $C_2$, $C_3$, and $C_4$ represent different crosslinking density. The typical absorptions of cellulose (curves of MCC and $C_0$) were observed at 3445 $cm^{-1}$ (O—H), 1064 $cm^{-1}$ (C—O of secondary alcohol), and 2893 $cm^{-1}$ (C—H), which were in accordance with an earlier work (Mormann & Michel, 2002). The spectra of regenerated cellulose ($C_0$) from DMAc/LiCl solvent system revealed no significant difference from MCC. A characteristic peak of amide (NHCO) at 1537 $cm^{-1}$ emerged (Gironès et al., 2007; Mormann & Michel, 2002) and signals at 1597 $cm^{-1}$, 1510 $cm^{-1}$ associated to the benzene rings of TDI structure (Gironès et al., 2007) can be obviously detected. Peaks at 1659 $cm^{-1}$, 1412 $cm^{-1}$, and 1311 $cm^{-1}$ were attributed to C=O stretching (amide: NHCOO), O—C=O stretching, and C—N stretching, respectively. Peaks around 3445 $cm^{-1}$ of $C_0$–$C_4$ which was attributed to OH group (Wilpiszewska & Spychaj, 2007), exhibited visible reduction with increasing amount of TDI, indicating that more OH groups were involved in reaction as more TDI added. And the peaks at 1200–1660 $cm^{-1}$ gradually strengthened simultaneously because more carbamate groups were created due to crosslinking, suggesting higher crosslinking density was obtained after introducing more TDI. No signal at 2265 $cm^{-1}$ (Stenstad, Andresen, Tanem, & Stenius, 2008) was detected indicating that there were no unreacted isocyanate groups remaining at the backbone of the polymer. All above data suggested that the reaction between MCC and TDI was successful and crosslinking density could be adjusted by controlling the amount of TDI.

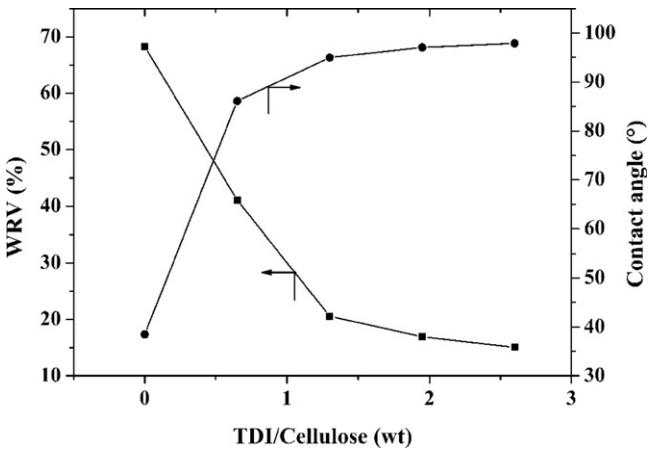


**Fig. 2.** WRVs and contact angles of cellulose films with different crosslinking density.

### 3.2. Hydrophobicity

The hydrophilicity/hydrophobicity is an important parameter to characterize surface properties which was closely related to the permeation and biodegradability. To investigate the influence of functionalization on the hydrophilicity/hydrophobicity of the modified films, WRVs and contact angles were examined (Fig. 2). Cellulose exhibits a high hygroscopicity arising from the interaction between its hydroxy groups and water molecules (Klemm et al., 1998, chap. 2), so measurement of WRVs can be used to characterize both hydrophilicity and crosslinking density. The WRV of $C_0$ agreed with results of earlier works (Klemm et al., 1998, chap. 2; Nishioka, Uno, & Kosai, 1990). With increasing amount of TDI, WRVs dropped sharply from 68.31% to 15.07%, indicating that adding of TDI enhanced the hydrophobicity of the films. As more hydrophobic TDI reacted to the hydroxy groups of cellulose, the network of the polymer became tightly, leading to the surface of the films being more hydrophobic and hindering water penetration into the films. Compared the WRVs of $C_2$ with $C_3$ and $C_4$, we can see that in $C_3$ and $C_4$, cellulose reacting with more TDI than in $C_2$ did not increase crosslinking density significantly and decrease hydrophilicity correspondingly. This may be explained that the network of $C_2$ was tight and water molecule was hard to penetrate into the film due to high crosslinking density, and further increase of crosslinking density can no longer influence the size of polymer network distinctly.

The contact angle measurement is a traditional method to characterize the hydrophobicity/hydrophilicity behavior of materials. From Fig. 2, it can be seen that contact angles increased from 38.5° to 97.9° as TDI content increasing, and the contact angle of $C_0$ was conformed to early investigations (Alila, Ferraria, Botelho do Rego, & Boufi, 2009; Siqueira et al., 2010). These results clearly demonstrated that the hydrophobicity of cellulose films was increased by crosslinking with more TDI. The results of contact angles corresponded fairly well with those of WRVs. Similar to WRVs, cellulose reacting with greater amount of TDI in $C_2$ did not increase hydrophobic property significantly probably due to the same reason mentioned above. Thus, the hydrophilicity/hydrophobicity of the cellulose films can be adjusted depending on our requirement.

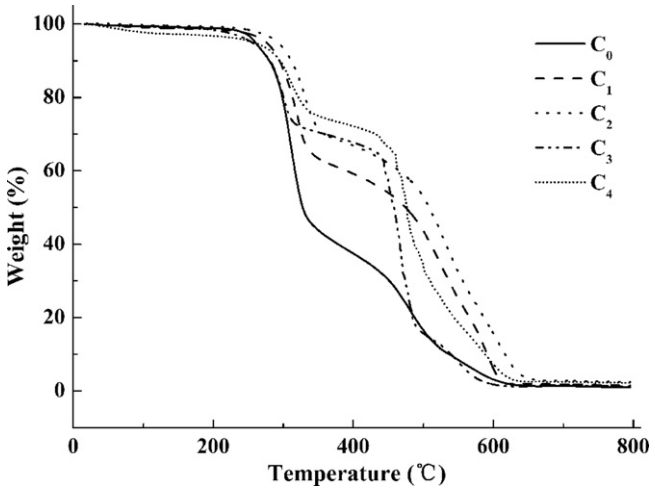


**Fig. 3.** TGA curves of TDI modified cellulose with different crosslinking density.

### 3.3. Thermal analysis

Thermal degradation properties of cellulose derivatives were investigated with TGA. From Fig. 3, it can be found that regenerated cellulose without TDI modification ($C_0$) demonstrated weight loss up to 58.37% at 280–330 °C, and this weight loss profile was in accordance with earlier works (Huang & Li, 1998; Jandura, Riedl, & Kokta, 2000; Mormann & Michel, 2002). The curve of $C_0$ can be roughly divided into two sections, ranging between 280–330 °C and 330–600 °C respectively, and the second section represented gradual weight loss than the first one, and the curve was almost identical with an early work (Ouajai & Shanks, 2005). This can be explained that the supramolecular structure of cellulose is interpreted by a two-phase model assuming low ordered ('amorphous') and highly ordered ('crystalline') regions (Klemm et al., 1998, chap. 2), and the amorphous region oxidized at lower temperature and higher speed, while the crystalline region oxidized at higher temperature and lower speed.

The TGA thermograms of crosslinked cellulose exhibited two sections as well, which was consistent to the previous published results (Duquesne et al., 2001). At the low temperature section (280–330 °C), weight loss rates of $C_1$–$C_4$ were 38.05%, 31.90%, 28.11%, 23.99% in contrast to 58.37% of $C_0$, which indicated that the materials were more heat-resisting as the crosslinking density increased. While in the high temperature section, the degradation rates of $C_1$–$C_4$ were higher than $C_0$. This behavior was probably because that the thermal behavior of crosslinked cellulose approached to polyurethane's as cellulose carbamate was formed, which displayed a rapid degradation during that range (Javni, Petrović, Guo, & Fuller, 2000). The results indicated the thermal stability of cellulose was remarkably improved by crosslinking with TDI.

### 3.4. Mechanical properties

Fig. 4 shows the mechanical properties of the films. The tensile strength, the Young's modulus, and the elongation at break of the films were unaminously improved with increased crosslinking density. The results were due to the formation of three-dimensional network structure by crosslinking between hydroxyl and isocyanate, which restricted the chains from sliding off one another and generated elasticity in cellulose (Bhattacharya, Rawlins, & Ray, 2009). Surprisingly, the elongation at break was also improved together with tensile strength and Young's modulus, indicating that the crosslinked cellulose membrane possessed extraordinary

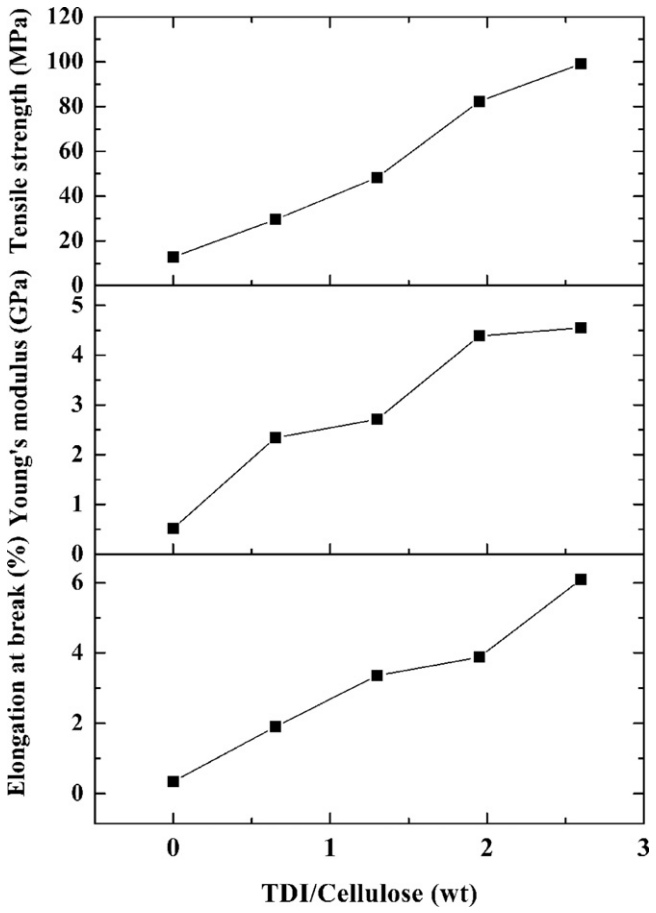


**Fig. 4.** Mechanical properties of TDI modified cellulose with different crosslinking density.

enhanced mechanical properties for further application. And the mechanical properties of the films were tunable by regulating the crosslinking densities as required.

### 3.5. Permeation properties

Fig. 5 shows the accumulated urea penetration across cellulose films and the variation of flux ($J$) at different weight ratio of TDI/cellulose. Comparing slightly crosslinked cellulose film ($C_1$) to non-crosslinked cellulose film ($C_0$), a sharp decrease of total release amount of urea in 10 h from 5939.8 mg to 2135.6 mg (Fig. 5(A)) and a dramatic declination of flux from 107.7 mg/(cm$^2$ h) to 39.8 mg/(cm$^2$ h) (Fig. 5(C)) were found. Compared to $C_1$, even marked reduction of urea permeability of $C_2$ (4.8 mg/(cm$^2$ h)) was observed, indicating that the crosslinking effect was still significant. But further increase of crosslinking density ($C_3$ and $C_4$) did not improve release property distinctly (Fig. 5(B)). These results validated the conclusions from the water absorption and contact angles that introducing hydrophobic TDI group into the cellulose increased hydrophobicity and crosslinking density of cellulose films.

The diffusion coefficient of cellulose is very sensitive to the moisture content: more water leads to faster diffusion (Topgaard & Söderman, 2001), and the shortened relaxation times ($T_2$) of water within fully swollen cellulosic fibers are dominated by proton exchange with accessible cellulose hydroxyl groups (Ibbett, Schuster, & Fasching, 2008). These results were attributed to the decrease of hydroxyl groups of cellulose films caused by crosslinking with hydrophobic TDI and led to less water content in the films,

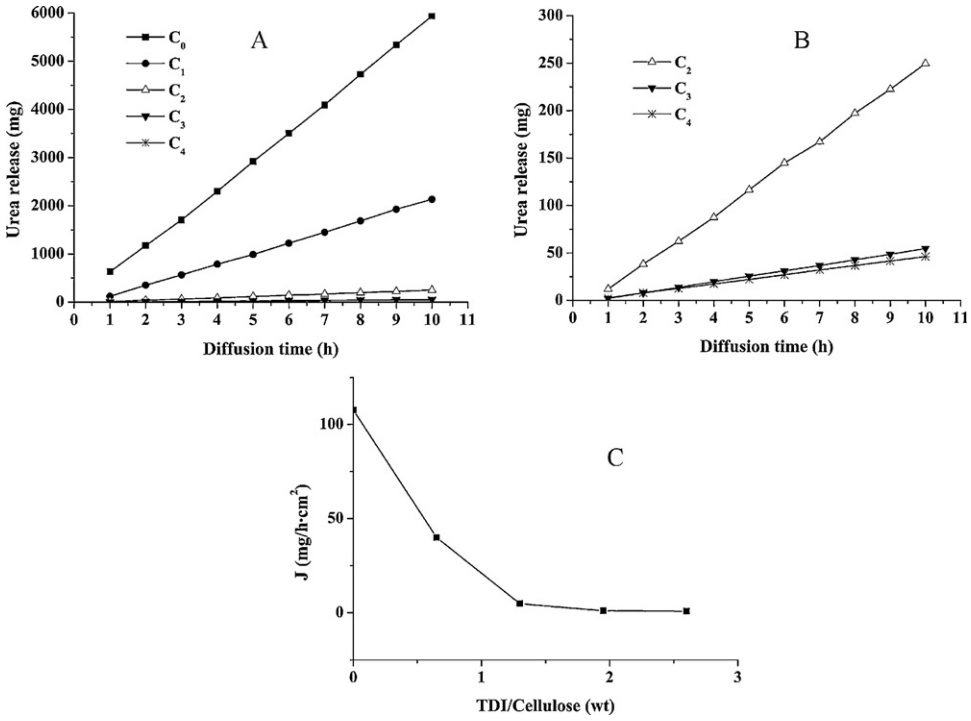


**Fig. 5.** Accumulated permeated urea of cellulose films with different crosslinking density, (A) $C_0$–$C_4$; and (B) $C_2$–$C_4$, magnification of (A) and variation of flux ($J$) with weight ratio of TDI and cellulose (C).

which slowed down the permeation of water soluble molecules, like urea. Moreover, the permeability is also depending on the microphase structures of the films (Nishioka, Tsuetaki, Kato, & Uno, 1994; Wu et al., 2010), mainly the free volume fraction (Valente et al., 2005). The linear structure of cellulose was converted into network structure due to crosslinking, which shrank the intermolecular space of the films and hindered migration of urea across films, thus the permeability of the films weakened as the crosslinking density increased, while the structure change of cellulose membranes in other works was due to blending with other polymer (Valente et al., 2005; Wu et al., 2010) or grafting (Nishioka et al., 1994). The morphology of the films didn't change after permeation experiments, and this meant the films retained their structure for further usage.

Furthermore, from Fig. 5(A and B), we can see that all curves are linear ($R^2 > 0.99$), suggesting the permeation rates of the films remain unchanged essentially. Since the films were fully swollen prior to the diffusion experiments, and the thickness of films and operating temperature were critically controlled in constant value, the diffusion rate of water molecules with dissolving urea through intermolecular space in the fully swollen state remained constant (Ibbett et al., 2008). The permeability also correlates to the solute molecular weight, higher molecular weight leading to lower permeability (Nishioka et al., 1994; Wu et al., 2010). Hence the characters of both the permeating solute and the films should be taken into consideration while the films are designed.

### 3.6. Degradation properties

The International Standard ISO 14852 (1999) was adopted for determining the aerobic biodegradability of the films. In this method, carbon conversion is an unequivocal indicator of biodegradation processes and can be measured precisely and reproducibly. Fig. 6 shows the accumulated $CO_2$ produced in the controlled composting test. All the samples had higher $CO_2$ emission than CK except in the case of PE, which is not biodegradable. This result indicated that microorganisms in composting test medium, mainly gram-positive cocci and gram-positive rods (Hassen et al., 2001), utilized the samples as extra carbon sources, and TDI modified cellulose films retained its biodegradability considerably. As demonstrated in Fig. 6, the biodegradability of cellulose films weakened as crosslinking density increasing, while in the cases of $C_3$ and $C_4$ with higher crosslinking density than $C_2$, the biodegradability showed no significant reduction.

Less than 5% residues remained at the fourth month for the non-crosslinking cellulose films ($C_0$, data not shown) from the cultivated soil burying experiment, suggesting the regenerated cellulose films possess fairly good biodegradability. Fig. 7 shows the SEM images of PE and crosslinked cellulose films before and after buried in soil for 12 months. The PE film (Fig. 7(A)), which is not biodegradable, showed no observable changes in terms of surface morphology. The

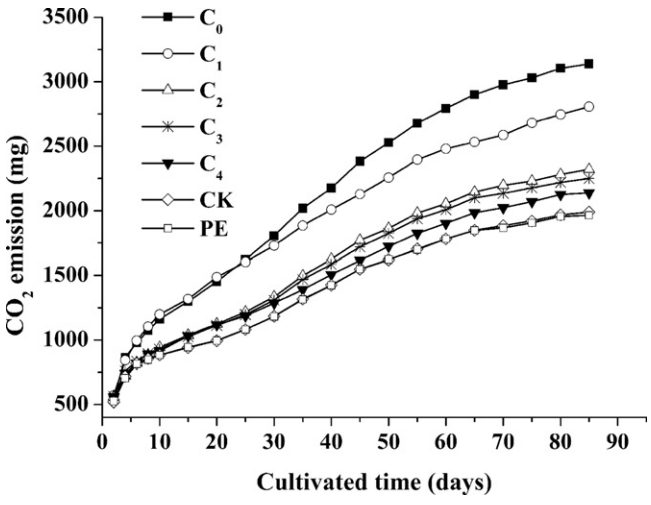


**Fig. 6.** Accumulated $CO_2$ produced in the controlled composting test.

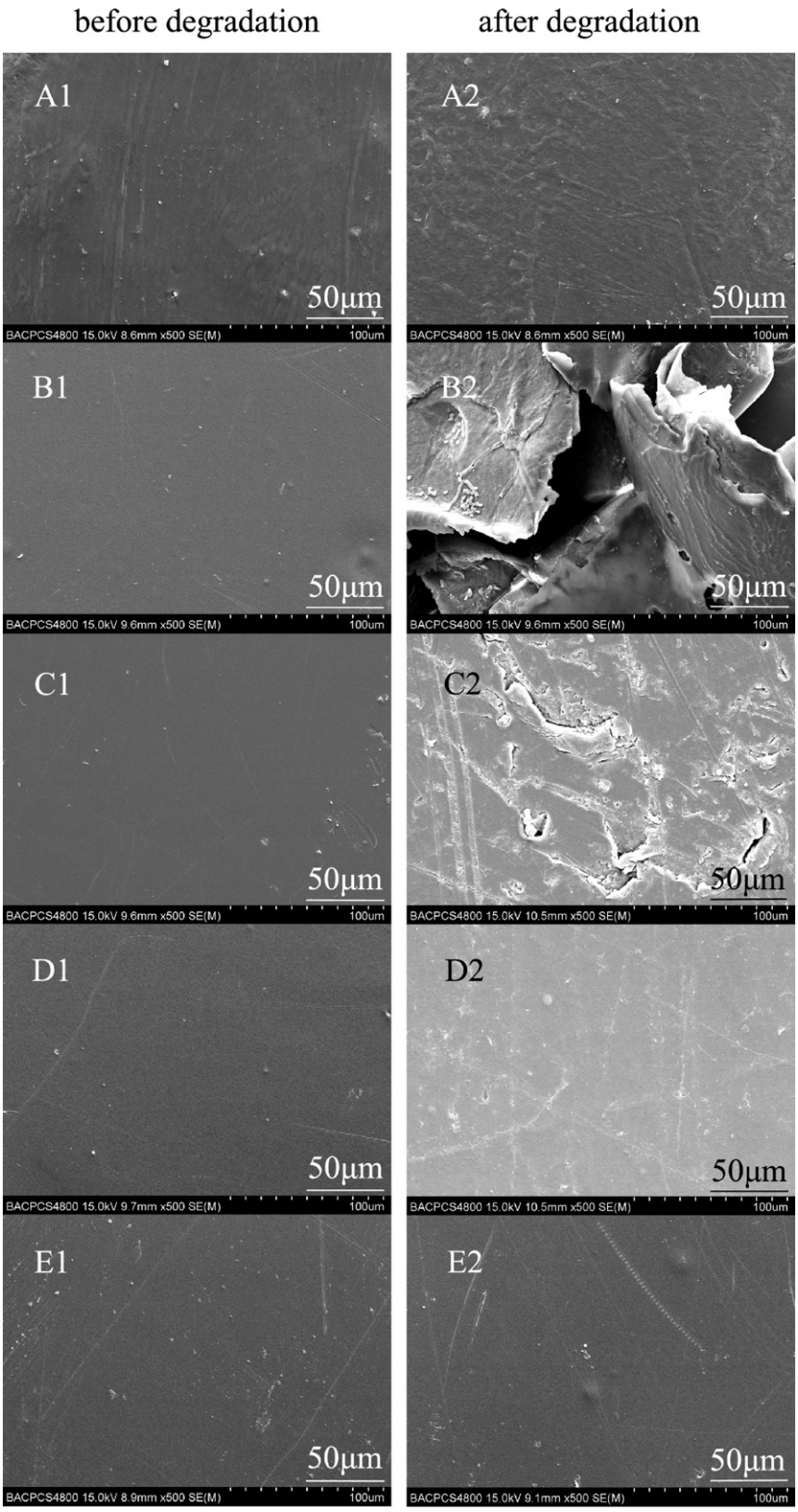


**Fig. 7.** SEM images of PE (A1, A2), $C_1$ (B1, B2), $C_2$ (C1, C2), $C_3$ (D1, D2), $C_4$ (E1, E2), before and after buried in natural cultivated soil for 12 months.

surfaces of crosslinked cellulose films before bury (Fig. 7(B1–E1)) were smooth and uniform, while the image of $C_1$ after degradation (Fig. 7(B2)) showed huge cracks and holes, even with pieces material stripping and suspending in the air. The image of $C_2$ after degradation (Fig. 7(C2)) showed small cracks and holes, and the surfaces of $C_3$ and $C_4$ were still flat and intact after degradation (Fig. 7(D2 and E2)). The results of weight losses after 12 months burying treatment were 0.17%, 7.49%, 1.23%, 0.34%, 0.42% for PE, $C_1$,

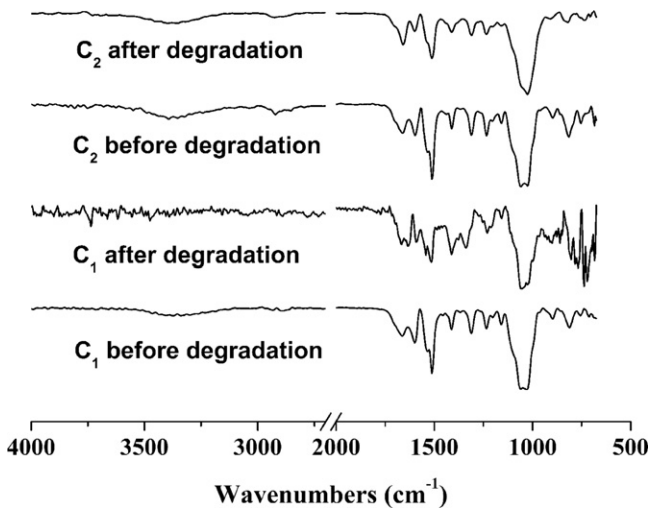


**Fig. 8.** ATR-IR spectra of $C_1$ (before and after degradation) and $C_2$ (before and after degradation).

$C_2$, $C_3$, $C_4$, respectively. The polymer was decomposed into small and soluble molecules by microorganisms in soil, and they were released from the films, resulting cracks and holes on the surfaces and weight losses of the films. The films with higher crosslinking densities, more hydrophobic and compact in structure, were more repellent to the microorganisms in soil, and thus retained in intact morphology and less weight losses. These results indicated that the modified cellulose films with higher crosslinking densities were less decomposable by microorganisms in soil, and this was confirmed by the results of ATR-IR spectra.

The ATR-IR spectra of $C_1$ and $C_2$ before and after degradation in natural cultivated soil for 12 months were exploited to further characterize degradation properties and shown in Fig. 8. In the case of $C_1$, a new absorption peak appeared at 1634 $cm^{-1}$ after degradation, representing anti-symmetric $COO^-$ stretching (Ouajai & Shanks, 2005), was probably due to the oxidation of hydroxy groups by soil microorganisms (Tomšič et al., 2007; Wilson, 2009). The weakening absorption peaks at 1598 $cm^{-1}$ and 1510 $cm^{-1}$ associated to the benzene rings of TDI structure (Gironès et al., 2007) demonstrated that some crosslinking bonds were broken down and TDI molecules dropped from the polymer backbone. The denticulate peaks in the range of 2500–4000 $cm^{-1}$ and 600–900 $cm^{-1}$ may be caused by the degradation products. The ATR-IR curve of $C_2$ showed no change except for peaks at 1598 $cm^{-1}$ and 1510 $cm^{-1}$, indicating that some TDI molecules came off from the skeleton too.

Cellulose is highly susceptible to microbial degradation (Tomšič et al., 2007), but after suitable modification it is resistant to microbial corrosion in varying degrees as demonstrated above and other works (Ouajai & Shanks, 2005; Tomšič et al., 2007). The degradation of cotton fibers by bacterial proceeds from the fiber surface toward the inner parts, and the degradation process needs for a high moisture, which requires the fabric to be saturated throughout the whole process of degradation (Clarke, 1997). In the experiment of composting incubation, all the films were immersed in the culture solution, where bacterial was the dominant microorganism, so hydrophobic films were more resistant to bacterial and presented less biodegradability. The result of the cultivated soil burying experiment agreed fairly well with that of controlled composting incubation experiment. The rate of the water molecule pervading the material influences the rate of degradation (Yuan et al., 2007), which would also explain that films with more hydrophobic properties and higher crosslinking densities possessed less biodegradability.

All the data above demonstrated that all the cellulose films with different crosslinking density were biodegradable, and more importantly the biodegradability of the films was tunable by adjusting the crosslinking densities of the films.

## 4. Conclusions

Cellulose films with different crosslinking density were prepared in homogeneous conditions. The hydrophobicity, thermal stability, and mechanical properties were improved after the TDI modifications. The urea permeation experiment demonstrated that the permeation properties of cellulose films were gradually enhanced by crosslinking. The biodegradability of the films was confirmed by the method of ISO 14852-1999 and examined in natural cultivated soil. The results of $CO_2$ emission, SEM, and ATR-IR indicated that the biodegradability decreased as the crosslinking density of cellulose films increased. The controlled permeation and biodegradability properties of cellulose films can be obtained by adjusting the crosslinking density.

## Acknowledgments

This work was supported by Chinese National Scientific Foundation (20875100 & 21175150); The New Century Excellent Talents in Universities (NCET-0810), by Ministry of Education of China; National Key Technology R&D Program (2011BAD11B02), by Ministry of Science & Technology of China.

## References

Alila, S., Ferraria, A. M., Botelho do Rego, A. M., & Boufi, S. (2009). Controlled surface modification of cellulose fibers by amino derivatives using N,N′-carbonyldiimidazole as activator. *Carbohydrate Polymers*, *77*, 553–562.

Amarasekara, A. S., & Owereh, O. S. (2009). Homogeneous phase synthesis of cellulose carbamate silica hybrid materials using 1-*n*-butyl-3-methylimidazolium chloride ionic liquid medium. *Carbohydrate Polymers*, *78*, 635–638.

Bhattacharya, A., Rawlins, J. W., & Ray, P. (2009). *Polymer grafting and crosslinking*. Hoboken: John Wiley & Sons, Inc.

Bodhibukkana, C., Srichanaa, T., Kaewnopparat, S., Tangthong, N., Bouking, P., Martin, G. P., et al. (2006). Composite membrane of bacterially-derived cellulose and molecularly imprinted polymer for use as a transdermal enantioselective controlled-release system of racemic propranolol. *Journal of Controlled Release*, *113*, 43–56.

Bras, J., Vaca-Garcia, C., Borredon, M.-E., & Glasser, W. (2007). Oxygen and water vapor permeability of fully substituted long chain cellulose esters (LCCE). *Cellulose*, *14*, 367–374.

Chen, S. Y., Zou, Y., Yan, Z. Y., Shen, W., Shi, S. K., Zhang, X., et al. (2009). Carboxymethylated-bacterial cellulose for copper and lead ion removal. *Journal of Hazardous Materials*, *161*, 1355–1359.

Clarke, A. J. (1997). *Biodegradation of cellulose: Enzymology and biotechnology*. Lancaster: Technomic Publishing Co., p. 272.

Conner, A. H. (1995). Size exclusion chromatography of cellulose and cellulose derivatives. In C. S. Wu (Ed.), *Handbook of size exclusion chromatography* (pp. 331–352). New York: Marcel Dekker.

Diamantoglou, M., Platz, J., & Vienken, J. (1999). Cellulose carbamates and derivatives as hemocompatible membrane materials for hemodialysis. *Artificial Organs*, *23*, 15–22.

Dupont, A. L. (2003). Cellulose in lithium chloride/N,N-dimethylacetamide, optimisation of a dissolution method using paper substrates and stability of the solutions. *Polymer*, *44*, 4117–4126.

Duquesne, S., Le Bras, M., Bourbigot, S., Delobel, R., Camino, G., Eling, B., et al. (2001). Thermal degradation of polyurethane and polyurethane/expandable graphite coatings. *Polymer Degradation and Stability*, *74*, 493–499.

Erkselius, S., & Karlsson, O. J. (2005). Free radical degradation of hydroxyethyl cellulose. *Carbohydrate Polymers*, *62*, 344–356.

French, A. D., Bertoniere, N. R., Brown, R. M., Chanzy, H., Gray, D., Hattori, K., et al. (2004). Cellulose. In A. Seidel (Ed.), *Kirk-othmer encyclopedia of chemical technology* (5th ed., pp. 360–394). New York: John Wiley & Sons, Inc.

Gironès, J., Pimenta, M. T. B., Vilaseca, F., Carvalho, A. J. F., Mutjé, P., & Curvelo, A. A. S. (2007). Blocked isocyanates as coupling agents for cellulose-based composites. *Carbohydrate Polymers*, *68*, 537–543.

Gironès, J., Pimenta, M. T. B., Vilaseca, F., Carvalho, A. J. F., Mutjé, P., & Curvelo, A. A. S. (2008). Blocked diisocyanates as reactive coupling agents: Application to pine fiber-polypropylene composites. *Carbohydrate Polymers*, *74*, 106–113.

Glaus, M. A., & Van Loon, L. R. (2008). Degradation of cellulose under alkaline conditions: New insights from a 12 years degradation study. *Environmental Science & Technology*, *42*, 2906–2911.

Grainger, D., & Hägg, M. B. (2007). Evaluation of cellulose-derived carbon molecular sieve membranes for hydrogen separation from light hydrocarbons. *Journal of Membrane Science, 306*, 307–317.
Hassen, A., Belguith, K., Jedidi, N., Cherif, A., Cherif, M., & Boudabous, A. (2001). Microbial characterization during composting of municipal solide waste. *Bioresource Technology*, *80*, 217–225.
Hu, K. L., Li, B. G., Lv, Y. Z., Duan, Z. Q., Li, Z. Z., Li, G. T., et al. (2006). Spatial variation of physico-chemical properties in Shangzhuang experimental station of China Agricultural University. *Journal of China Agricultural University*, *11*, 27–33 (In Chinese).
Huang, M. R., & Li, X. G. (1998). Thermal degradation of cellulose and cellulose esters. *Journal of Applied Polymer Science*, *68*, 293–304.
Ibbett, R. N., Schuster, K. C., & Fasching, M. (2008). The study of water behaviour in regenerated cellulosic fibres by low-resolution proton NMR. *Polymer*, *49*, 5013–5022.
International Standard ISO 14852. (1999). *Determination of the ultimate aerobic biodegradability of plastic materials in an aqueous medium – Method by analysis of evolved carbon dioxide*.
Jandura, P., Riedl, B., & Kokta, B. V. (2000). Thermal degradation behavior of cellulose fibers partially esterified with some long chain organic acids. *Polymer Degradation and Stability*, *70*, 387–394.
Javni, I., Petrović, Z. S., Guo, A., & Fuller, R. (2000). Thermal stability of polyurethanes based on vegetable oils. *Journal of Applied Polymer Science*, *77*, 1723–1734.
Jawaid, M., & Khalil, H. P. S. A. (2011). Cellulosic/synthetic fibre reinforced polymer hybrid composites: A review. *Carbohydrate Polymers*, *86*, 1–18.
Khan, F. Z., Shiotsuki, M., Nishio, Y., & Masuda, T. (2008). Synthesis, characterization, and gas permeation properties of *t*-butylcarbamates of cellulose derivatives. *Journal of Membrane Science*, *312*, 207–216.
Klemm, D., Philipp, B., Heinze, T., Heinze, U., & Wagenknecht, W. (1998). *Comprehensive cellulose chemistry volume I: Fundamentals and analytical methods*. Weinheim: WILEY-VCH Verlag GmbH.
Liu, S. L., Zeng, J., Tao, D. D., & Zhang, L. N. (2010). Microfiltration performance of regenerated cellulose membrane prepared at low temperature for wastewater treatment. *Cellulose*, *17*, 1159–1169.
Łojewski, T., Sawoszczuk, T., Łagan, J. M., Zięba, K., Barański, A., & Łojewska, J. (2010). Furfural as a marker of cellulose degradation. A quantitative approach. *Applied Physics A: Materials Science & Processing*, *100*, 873–884.
Lqbal, J., Kim, H. J., Yang, J. S., Baek, K., & Yang, J. W. (2007). Removal of arsenic from groundwater by micellar-enhanced ultrafiltration (MEUF). *Chemosphere*, *66*, 970–976.
Mormann, W., & Michel, U. (2002). Improved synthesis of cellulose carbamates without by-products. *Carbohydrate Polymers*, *50*, 201–208.
Nishioka, N., Tsuetaki, M., Kato, R., & Uno, M. (1994). Permeability through cellulose membranes grafted with vinyl monomers in a homogeneous system. VIII. N-vinylpyrrolidone-grated cellulose membranes. *Journal of Applied Polymer Science*, *52*, 959–966.
Nishioka, N., Uno, M., & Kosai, K. (1990). Permeability through cellulose membranes grafted with vinyl monomers in a homogeneous system. VII. Acrylamide grafted cellulose membranes. *Journal of Applied Polymer Science*, *41*, 2857–2868.
Ouajai, S., & Shanks, R. A. (2005). Composition, structure and thermal degradation of hemp cellulose after chemical treatments. *Polymer Degradation and Stability*, *89*, 327–335.
Pala, H., Mota, M., & Gama, F. M. (2007). Enzymatic depolymerisation of cellulose. *Carbohydrate Polymers*, *68*, 101–108.
Pan, J., Hamad, W., & Straus, S. K. (2010). Parameters affecting the chiral Nematic phase of nanocrystalline cellulose films. *Macromolecules*, *43*, 3851–3858.
Philipp, B., & Schempp, W. (2009). Progress in cellulose research in the reflection of the zellcheming cellulose symposium. *Macromolecular Symposia*, *280*, 4–14.
Schmitt, F., Granet, R., Sarrazin, C., Mackenzie, G., & Krausz, P. (2011). Synthesis of anion exchange membranes from cellulose: Crosslinking with diiodobutane. *Carbohydrate Polymers*, *86*, 362–366.
Siqueira, G., Bras, J., & Dufresne, A. (2010). New process of chemical grafting of cellulose nanoparticles with a long chain isocyanate. *Langmuir*, *26*, 402–411.
Stenstad, P., Andresen, M., Tanem, B. S., & Stenius, P. (2008). Chemical surface modifications of microfibrillated cellulose. *Cellulose*, *15*, 35–45.
Tatárová, I., Fáberb, R., Denoyelc, R., & Polakoviča, M. (2009). Characterization of pore structure of a strong anion-exchange membrane adsorbent under different buffer and salt concentration conditions. *Journal of Chromatography A*, *1216*, 941–947.
Tian, Y., Wu, M., Liu, R. G., Li, Y. X., Wang, D. Q., Tan, J. J., et al. (2011). Electrospun membrane of cellulose acetate for heavy metal ion adsorption in water treatment. *Carbohydrate Polymers*, *83*, 743–748.
Tomšič, B., Simončič, B., Orel, B., Vilčnik, A., & Spreizer, H. (2007). Biodegradability of cellulose fabric modified by imidazolidinone. *Carbohydrate Polymers*, *69*, 478–488.
Topgaard, D., & Söderman, O. (2001). Diffusion of water absorbed in cellulose fibers studied with $^{1}$H-NMR. *Langmuir*, *17*, 2649–2702.
Valente, A. J. M., Burrows, H. D., Polishchuk, A. Y., Domingues, C. P., Borges, O. M. F., Eusebio, M. E. S., et al. (2005). Permeation of sodium dodecyl sulfate through polyaniline-modified cellulose acetate membranes. *Polymer*, *46*, 5918–5928.
Wang, Y. J., Yang, L. G., Luo, G. S., & Dai, Y. Y. (2009). Preparation of cellulose acetate membrane filled with metal oxide particles for the pervaporation separation of methanol/methyl *tert*-butyl ether mixtures. *Chemical Engineering Journal*, *146*, 6–10.
Wilpiszewska, K., & Spychaj, T. (2007). Chemical modification of starch with hexamethylene diisocyanate derivatives. *Carbohydrate Polymers*, *70*, 334–340.
Wilson, D. B. (2009). Evidence for a novel mechanism of microbial cellulose degradation. *Cellulose*, *16*, 723–727.
Wu, J. J., Liang, S. M., Dai, H. G., Zhang, X. Y., Yu, X. L., Cai, Y. L., et al. (2010). Structure and properties of cellulose/chitin blended hydrogel membranes fabricated via a solution pre-gelation technique. *Carbohydrate Polymers*, *79*, 677–684.
Yuan, W. Z., Yuan, J. Y., Zhang, F. B., & Xie, X. M. (2007). Syntheses, characterization, and in vitro degradation of ethyl cellulose-*graft*-poly (*ε*-caprolactone)-*block*-poly (l-lactide) copolymers by sequential ring-opening polymerization. *Biomacromolecules*, *8*, 1101–1108.
Zaghbani, N., Hafiane, A., & Dhahbi, M. (2007). Separation of methylene blue from aqueous by micellar enhanced ultrafiltration. *Separation and Purification Technology*, *55*, 117–124.
Zou, X. J., Wang, Z. X., Dai, X. M., Zhou, Y., & Ma, X. J. (2006). Rate of controlled release urea pervasion through membrane determined by ultraviolet spectrophotometry. *Spectroscopy and Spectral Analysis*, *26*, 1151–1154 (In Chinese).